Thermodynamics−Structure Relationship of Single Mismatches in RNA/DNA Duplexes†

Naoki Sugimoto,*,‡,§ Mariko Nakano,‡,|| and Shu-ichi Nakano‡,||

Department of Chemistry, Faculty of Science, and High Technology Research Center, Konan University, 8-9-1 Okamoto, Higashinada-ku, Kobe 658-8501, Japan

Received April 11, 2000; Revised Manuscript Received June 26, 2000

ABSTRACT: Thermodynamics of 66 RNA/DNA duplexes containing single mismatches were measured by UV melting methods. Stability enhancements for rG·dT mismatches were the largest of all mismatches examined here, while rU·dG mismatches were not as stable. The methyl group on C5 of thymine enhanced the stability by 0.12 ∼ 0.53 kcal mol^{-1} depending on the identity of adjacent Watson−Crick base pairs, whereas the 2′-hydroxyl group in ribouridine stabilized the duplex by ∼0.6 kcal mol^{-1} regardless of the adjacent base pairs. Stabilities induced by the methyl group in thymine, the 2′-hydroxyl group of ribouridine, and an nucleotide exchange at rG·dT and rU·dG mismatches were found to be independent of each other. The order for the mismatch stabilities is rG·dT ≫ rU·dG ≈ rG·dG > rA·dG ≈ rG·dA ≈ rA·dC > rA·dA ≈ rU·dT ≈ rU·dC > rC·dA ≈ rC·dT, although the identity of the adjacent base pairs slightly altered the order. The pH dependence stability and structural changes were suggested for the rA·dG but not for rG·dA mismatches. Comparisons of trinucleotide stabilities for G·T and G·U pairs in RNA, DNA, and RNA/DNA duplexes indicate that stable RNA/DNA mismatches exhibit a stability similar to RNA mismatches while unstable RNA/DNA mismatches show a stability similar to that of DNA mismatches. These results would be useful for the design of antisense oligonucleotides.

Thermodynamics of mismatches in RNA and DNA duplexes have been investigated due to their importance in the secondary structure prediction (*1*, *2*), the understanding of misincorporation of bases during replication (*3*), and the development of hybridization techniques (*4*, *5*). It has also been found that unusual structures of mismatch bases are related to ribozyme activities (*6*−*8*) and protein recognition (*9*, *10*). Studies of mismatched thermodynamics and structures are not complete due to a large number of possible combinations for mismatches, although there have been many reports for Watson−Crick base pairs (*11*−*17*). Nevertheless, thermodynamics for RNA single mismatches (*18*−*23*), RNA tandem mismatches (*24*−*30*), and DNA single mismatches (*15*, *16*, *31*−*35*) have been investigated systematically. Single rG·rU mismatches in RNA duplexes and dG·dU mismatches in DNA duplexes can form stable wobble base pairs (*36*, *37*) that are almost as stable as rA·rU and dA·dT Watson−Crick base pairs (*11*, *15*, *17*). Except for the rG·rU mismatches, stability enhancements for RNA single mismatches ranged from −2.6 to 1.7 kcal mol^{-1} at 37 °C, and rG·rU, rG·rG, and rU·rU mismatches exhibited higher stabilities that were influenced by adjacent Watson−Crick base pairs (*23*). Tandem mismatches have been the subject of several prior studies that showed the stabilizing mismatches to be rG·rU, rG·rA, and rU·rU (*1*). Thermodynamics of DNA single mismatches have been studied systematically, and prediction parameters based on the nearest-neighbor model are suggested for every possible single mismatch including stable ones such as dG·dG, dG·dT, and dG·dA (*15*, *32*−*35*).

Hydrogen bond formation between mismatched nucleotides are found for some mismatches as well as wobble base pairs. Four kinds of conformations have been reported for G·A mismatched pairs that appeared to be affected by the number of mismatches, the identity of adjacent base pairs, and pH (*36*−*41*). Single G·G pairs are relatively stable in single RNA (*23*) and DNA mismatches (*35*), and imino proton NMR revealed dG·dG involving hydrogen bonding (*35*). C·A mismatches can form two hydrogen bonds when N1 of A is protonated at low pH (*34*, *42*, *43*). On the basis of the difference of the stabilities of single and tandem mismatches in RNA duplexes, it is speculated that the mismatch environments also affect the mismatch conformation (*23*). Obviously, more studies for mismatches are necessary to know the structure−stability relationship for mismatches in duplexes.

RNA duplexes form A-type conformation characterized by C3′-*endo* sugar puckers in aqueous solution, while DNA duplexes adopt a B-form with C2′-*endo* puckers (*44*). The axial rise and the rotation from one residue to the next are also different; 2.56 Å and 32.7° for the A-RNA and 3.38 Å and 36.0° for the B-DNA, respectively (*44*). CD, X-ray crystallographic, and NMR studies revealed that RNA/DNA duplexes showed an A-like conformation with the RNA

* To whom correspondence should be addressed. Phone: +81-78-435-2497, Fax: +81-78-435-2539, E-mail: sugimoto@konan-u.ac.up.

† This work was supported in part by Grants-in-Aid for Scientific Research from the Ministry of Education, Science, Sports and Culture, Japan, and a grant from "Research for the Future" program of the Japan Society for the Promotion of Science.

‡ Department of Chemistry, Faculty of Science, Konan University.

§ High Technology Research Center, Konan University.

|| Present address: Department of Chemistry, The Pennsylvania State University, University Park, Pennsylvania 16802, USA.

10.1021/bi000819p CCC: $19.00
Published on Web 08/23/2000

strand adopting C3′-*endo* sugar puckers, and the DNA strand was more flexible (*45*) and had an equilibrium between C2′- and C3′-*endo* sugar puckers (*46*). Since most RNA/DNA duplexes can adopt an intermediate structure between A- and B-type conformation, structure−stability relationship for mismatches can be available by comparing to previous mismatch data reported for A-RNA and B-DNA duplexes.

In this study, we measured thermodynamics of 52 RNA/DNA duplexes containing single mismatches of rA·dA, rA·dC, rA·dG, rC·dA, rC·dT, rG·dA, rG·dG, rG·dT, rU·dC, rU·dG, or rU·dT that are important in biological systems. Trinucleotide parameters are provided by this work, and stable mismatches are assigned. These parameters would be useful for the design of antisense nucleotides that have less hybridization ability with nontarget regions. Since it has been found that rG·dT mismatches are always more stable than rG·dU mismatches, we also quantified the energy contributions from the methyl group in C5 of thymine and the 2′-hydroxyl group in ribose by measuring an additional 12 duplexes including rG·dU, dU·dG, or dT·dG mismatches. Finally, trinucleotide parameters are compared for RNA, DNA, and RNA/DNA duplexes, and the stability−structure relationships of single mismatches in RNA/DNA duplexes are suggested.

EXPERIMENTAL PROCEDURES

Material Preparations. All oligodeoxyribonucleotides and oligoribonucleotides were synthesized chemically on a solid support and purified with reversed-phase HPLC as described previously (*12*). Final purity of oligomers was confirmed to be >98%. All nucleotides were desalted with a C-18 Sep-Pak cartridge before use. Each oligonucleotide concentration was determined by the absorbance at 260 nm, and the single strand extinction coefficients were determined via mono- and dinucleotides (*47*). Average values of RNA and DNA extinction coefficients were used as extinction coefficients for sequences containing RNA−DNA chimera junctions. All duplexes were prepared by mixing two strands of equimolar concentrations.

UV Measurements. Absorbances were measured with a Hitachi U-3200 and U-3210 equipped with Hitachi SPR-7 and SPR-10 thermoprogrammers. The water condensation on the cuvette exterior at a low temperature range was avoided by flushing with a constant stream of dry N_2 gas. The heating rate was 0.5 or 1.0 °C/min. UV[1] melting curves were measured in an NaCl-phosphate buffer containing 1 M NaCl, 10 mM Na_2HPO_4, and 1 mM Na_2EDTA adjusted to pH 7.0, or 1 M NaCl, 10 mM NaH_2PO_4, and 1 mM Na_2-EDTA adjusted to pH 5.0 (*19*). Prior to the experiment, all buffers were degassed by heating to 90 °C for 10 min.

All melting curves were fitted with a theoretical equation to obtain thermodynamic parameters for double helix formation ($\Delta H°$, $\Delta S°$, and $\Delta G°_{37}$) as described elsewhere (*12*, *13*, *48*). We also evaluated these thermodynamics from T_m^{-1} vs $\ln(C_t/4)$ plots. From the slope and intercept of the inverse of a melting temperature, thermodynamic parameters were deduced with eqs 1 and 2:

$$T_m^{-1} = R \ln(C_t/4)/\Delta H° + [\Delta S°/\Delta H°] \quad (1)$$

$$\Delta G°_{37} = \Delta H° - (310.15)\Delta S° \quad (2)$$

where R is the gas constant and C_t is the total strand concentration.

Errors for these thermodynamics ($\sigma_{\Delta H°}$, $\sigma_{\Delta S°}$, and $\sigma_{\Delta G°_{37}}$) in a curve-fitting procedure were estimated as standard deviations from melting curves measured at different C_t values (at least eight different concentrations with 80 ∼ 0.8 μM). $\sigma_{\Delta H°}$ and $\sigma_{\Delta S°}$ for T_m^{-1} vs $\ln(C_t/4)$ methods were estimated from a linearity of the plots and $\sigma_{\Delta G°_{37}}$ was calculated by eq 3 (*15*, *17*).

$$(\sigma_{\Delta G°_{37}})^2 = (\sigma_{\Delta H°})^2 + (310.15)^2(\sigma_{\Delta S°})^2 - 2(310.15)(R_{\Delta H°,\Delta S°})\sigma_{\Delta H°}\sigma_{\Delta S°} \quad (3)$$

where $R_{\Delta H°,\Delta S°}$ is the correlation coefficient between $\Delta H°$ and $\Delta S°$. Thermodynamic parameters used in this study are the average values obtained from the curve-fitting and T_m^{-1} vs $\ln(C_t/4)$ plots, and error values represent the difference of thermodynamics determined by these two independent methods. In most cases, the differences of $\Delta G°_{37}$, $\Delta H°$, and $\Delta S°$ determined by the two methods are ± 0.1 kcal mol^{-1}, ± 3 kcal mol^{-1}, and ± 8 cal mol^{-1} K^{-1}, respectively.

Thermodynamics of Trinucleotide Formations Containing Mismatch Nucleotides. Thermodynamic parameters for single mismatch formation were calculated based on a nearest-neighbor model. Since the thermodynamics of a single mismatch are significantly affected by adjacent Watson−Crick base pairs, we considered trinucleotides involving a single mismatch pair and nearest-neighbor base pairs. The stability of trinucleotides involving mismatches can be calculated using a stability of a duplex that does not include the mismatch and a nearest-neighbor stability of base pairs adjacent to the mismatch. For example, a rN·dN′ mismatch pair closed by rC·dG and rG·dC base pairs is calculated as follows (*12*, *23*, *27*): $\Delta G°_{37}$(rC$\underline{\text{N}}$G/dC$\underline{\text{N}'}$G) = $\Delta G°_{37}$(rAAGC$\underline{\text{N}}$GUAG/dCTAC$\underline{\text{N}'}$GCTT) − $\Delta G°_{37}$(rAAGCGUAG/dCTAC$\underline{\text{G}}$CTT) + $\Delta G°_{37}$(r$\underline{\text{C}}$G/dCG). Error values for trinucleotide parameters were calculated from square-root errors of each terms. Estimated errors in $\Delta G°_{37}$, $\Delta H°$, and $\Delta S°$ are ± 0.22 kcal mol^{-1}, ± 3 kcal mol^{-1}, and ± 8 cal mol^{-1} K^{-1}, respectively.

CD Measurements. CD spectra were obtained on a JASCO J-600 spectropolarimeter equipped with a temperature controller. The experimental temperature was 5 °C. The cuvette-holding chamber was flushed with a constant stream of dry N_2 gas to avoid water condensation on the cuvette exterior. All CD spectra were measured from 320 to 200 nm in 0.1-cm path length cuvette.

Molecular Modeling. QUANTA 97.1 SEQUENCE BUILDER was used to generate DNA and RNA based on the DNA.RTF and RNA.RTF topology data prepared for CHARMm version 23.2 (Molecular Simulations Inc.). An initial structure of RNA/DNA hybrids was built with "Nucleic Acids Builder" in QUANTA 97.1. All molecular mechanics calculations were performed with CHARMm version 23.2. Energy of the structure was minimized by the adopted basis set Newton−Raphson (ABNR) method. The parameters for constraints of dihedral angles and distance

[1] Abbreviations: UV, ultraviolet; CD, circular dichroism; HPLC, high-performance liquid chromatography; T_m, melting temperature; Na_2-EDTA, disodium ethylenediaminetetraacetate.

of C1′−C1′ were regarded as nearly A-form. The constraints used were ±10° and ±0.2 Å range for dihedral angles and distances, respectively (*44*). The obtained structure was further minimized with its total internal (bond, angle, and dihedral energy) and external energy (improper, Lennard−Jones, and electrostatic energy) by the adopted basis set Newton−Raphson (ABNR) method. All calculations were performed on a Silicon Graphics Indigo2 workstation running IRIX 5.3.

RESULTS

Stabilities of Single Mismatches in RNA/DNA Duplexes. It has been reported that thermodynamics of RNA and DNA duplexes containing single mismatches depend on the identity of the mismatch and the Watson−Crick base pairs adjacent to the mismatched nucleotides (*15*, *16*, *18*−*23*, *31*−*35*). For RNA/DNA duplexes, two mismatches are different when the mismatch nucleobases are exchanged, although it is not be considered for RNA and DNA homoduplexes For example, G·A mismatches can be constructed for rG·dA and rA·dG pairs (where rG·dA means a guanine−adenine mismatch with riboguanosine in the RNA strand and deoxyadenosine in the DNA strand in an RNA/DNA duplex). Thermodynamics of these two mismatches are expected to be different because stacking interactions and the influence from 2′-hydroxyl groups in RNA strands should change. To quantify the effects of mismatches in RNA/DNA duplexes, we examined 52 RNA/DNA duplexes containing either rA·dA, rA·dC, rA·dG, rC·dA, rC·dT, rG·dA, rG·dG, rG·dT, rU·dC, rU·dG, or rU·dT mismatched pairs. RNA/DNA duplexes used here were of the forms rAAGCNGUAG·dCTACN′GCTT, rUCACNCUAG·dCTAGN′GTGA, rUGAGNGUAC·dGTACN′CTCA, and rUUGGNCACC·dGGTGN′CCAA, where rN·dN′ represents the mismatched pair, and the underline is the trinucleotide that contains the mismatch and the adjacent base pairs. Thermodynamics obtained by UV melting curves are listed in Table 1. All the duplexes showed a two-state transition, and thermodynamic parameters used in this study were the average values obtained from curve fittings and T_m^{-1} vs ln(C_t/4) plots.

Thermodynamic parameters for a single mismatch in RNA/DNA duplexes were significantly affected by both the identity of the mismatch and the adjacent base pairs; differences of the duplex stability at 37 °C ($\Delta\Delta G°_{37}$) were more than 4 kcal mol^{-1} depending on the mismatch and adjacent base pairs (Table 1). The rG·dT mismatches enhanced the duplex stability more effectively than those of rC·dA and rC·dT. The data in Table 1 also revealed different thermodynamics for duplexes in which the mismatched nucleotides were exchanged from rN·dN′ to rN′·dN. The rG·dT containing duplexes were always more stable than those of rU·dG. For example, duplex stability of rAAGCGGUAG/dCTACTGCTT and rAAGCUGUAG·dCTACGGCTT was −8.57 and −6.41 kcal mol^{-1}, respectively, which have the same adjacent base pairs (as refered by trinucleotides of rCGG/dCTG and rCUG/dCGG). Moreover, rUUGGGCACC/dGGTGTCCAA was 1.22 kcal mol^{-1} more stable than rUUGGUCACC/dGGTGGCCAA. Enthalpy and entropy changes for these duplexes were also different. Effects of adjacent base pairs on the mismatch thermodynamics are also presented in Table 1. For example, when rG·dT mismatches were incorporated into rUUAACUGGC·dGCCAGTTAA at different locations, rUUAAGCUGGC/dGCCAGTTTAA showed the highest stability (−8.89 kcal mol^{-1}) which was 0.93 kcal mol^{-1} more stable than rUUAGACUGGC/dGCCAGTTTAA in which the rG·dT mismatch was flanked by two rA·dT pairs. For rU·dG mismatches, rUUAUACUGGC/dGCCAGTGTAA and rUUAAUCUGGC/dGCCAGGTTAA were the most stable (−7.46 kcal mol^{-1}), while rUUAACUUGGC/dGCCGAGTTAA was the least stable duplex (−6.60 kcal mol^{-1}). From these examples, it is obvious that systematic experiments and quantitative treatments are required to elucidate the effect of mismatch effects on the RNA/DNA duplex stabilities as described below.

Effects of the Methyl Group of Thymine and the 2′-Hydroxyl Group on the Stability of G·U and G·T Mismatches. Since thermodynamics of rG·dT and rU·dG mismatches were quite different even for duplexes having identical adjacent base pairs, we focused on the stabilities of rG·dT and rU·dG mismatches. It is possible that the effects of the 2′-hydroxyl group in ribose could be different for these two mismatches since uracil lacks the methyl group on C5 of thymine. We thus constructed 12 additional RNA/DNA duplexes that could form a Wobble base pair containing deoxyuridine (dU) in either an RNA or DNA strand to make rG·dU or dU·dG, or deoxythymidine (dT) in an RNA strand to make a dT·dG mismatch in RNA/DNA duplexes. Although insertions of dU·dG and dT·dG mismatches in RNA/DNA duplexes made RNA−DNA chimeric junctions, CD spectra revealed that these mismatches did not change the duplex structure as a whole (data not shown). Thermodynamics of these mismatches are listed in Table 2. Replacing uridine by thymine in a DNA strand (from rG·dU to rG·dT) invariably increased the stability by 0.12 ∼ 0.53 kcal mol^{-1}. Moreover, dT·dG mismatches were 0.21 ∼ 0.38 kcal mol^{-1} more stable than dU·dG mismatches. Accordingly, the methyl group in thymine raised all duplex stabilities examined here. However, enthalpy and entropy changes of the contributions from the methyl group were different. Replacing uridine by thymine in rUUGGGCACC/dGGTGUCCAA showed positive $\Delta\Delta H°$ and $T\Delta\Delta S°$ values but that in rUUGG(dU)CACC/dGGTGGCCAA showed negative $\Delta\Delta H°$ and $T\Delta\Delta S°$ contributions, although $\Delta\Delta G°_{37}$ are negative by the methyl group addition for both cases.

Effects of 2′-hydroxyl group were estimated from the energy differences between rU·dG and dU·dG in RNA/DNA duplexes. The results indicate that the 2′-hydroxyl group of rU stabilized the duplexes by 0.57 ∼ 0.63 kcal mol^{-1}, which was almost the same among four duplexes containing different adjacent base pairs. The enthalpy and entropy changes by the 2′-hydroxyl group ($\Delta\Delta H°$ and $T\Delta\Delta S°$) were also similar (−7.8 ∼ −9.0 kcal mol^{-1} and −23.5 ∼ −27.1 cal mol^{-1} K^{-1}, respectively). Thus, the stabilization by the 2′-hydroxyl group in rU was unaffected by the identity of adjacent base pairs, unlikely to the observations for the methyl group effects in thymine.

pH Effects for rG·dA and rA·dG Mismatches on the Stability and the Structure. Four conformations are found for G·A mismatch pairs in RNA and DNA duplexes (*32*, *38*−*41*), and one of them, A$^+$(*anti*)·G(*syn*), requires a protonation at N1 of adenine to form a hydrogen bonding with N7 of guanine, and the C1′−C1′ distance is ∼10.7 Å which is similar to those of Watson−Crick base pairs (10.4−10.7 Å). Thus, we investigated the influence of pH on the

Table 1: Thermodynamics of Duplex Formation of RNA/DNA Hybrids Containing an Internal Mismatch Base Pair[a]

	T_m^{-1} vs log C_t parameters				curve fit parameters			
RNA/DNA duplex	$-\Delta G°_{37}$ (kcal/mol)	$-\Delta H°$ (kcal/mol)	$-\Delta S°$ (cal/mol·K)	T_m[b] (°C)	$-\Delta G°_{37}$ (kcal/mol)	$-\Delta H°$ (kcal/mol)	$-\Delta S°$ (cal/mol·K)	T_m[b] (°C)
core sequences								
rAAGCGUAG[c]	7.7	66.6	190	42.4	7.9	67.8	193	43.6
dTTCGCATC								
rUCACCUAG	6.41 ± 0.42	59.4 ± 3.0	170.9 ± 8.9	36.3	6.46 ± 0.08	56.4 ± 1.1	161.0 ± 3.6	36.7
dAGTGGATC								
rUGAGGUAC	9.02 ± 0.32	71.1 ± 2.4	200.3 ± 7.0	48.1	9.07 ± 0.19	67.0 ± 1.0	186.9 ± 3.5	49.0
dACTCCATG								
rUUGGCACC[c]	8.7	57.0	156	48.8	8.8	55.3	150	50.1
dAACCGTGG								
rUUAACUGGC[c]	8.9	69.1	194	48.2	8.9	65.5	183	47.8
dAATTGACCG								
rA·dA mismatches								
rAAGC**A**GUAG	4.95 ± 0.09	58.1 ± 1.3	171.2 ± 4.0	29.1	5.10 ± 0.17	54.8 ± 1.9	160.2 ± 6.7	29.2
dTTCG**A**CATC								
rUCAC**A**CUAG	3.99 ± 0.32	42.6 ± 2.3	124.5 ± 6.9	19.5	3.71 ± 0.38	44.5 ± 3.0	131.4 ± 9.8	18.7
dAGTG**A**GATC								
rUGAG**A**GUAC	5.92 ± 0.20	67.4 ± 2.0	198.1 ± 6.1	34.4	5.87 ± 0.37	69.6 ± 8.8	205.4 ± 28.6	34.2
dACTC**A**CATG								
rUUGG**A**CACC	5.71 ± 0.41	45.3 ± 2.6	127.6 ± 7.5	31.6	5.62 ± 0.11	48.4 ± 2.5	137.8 ± 8.2	31.5
dAACC**A**GTGG								
rA·dC mismatches								
rAAGC**A**GUAG	5.07 ± 0.10	70.0 ± 1.6	209.3 ± 5.0	30.7	5.11 ± 0.56	64.9 ± 2.0	192.7 ± 6.6	30.5
dTTCG**C**CATC								
rUCAC**A**CUAG	4.97 ± 0.14	42.3 ± 1.3	120.4 ± 3.8	25.9	4.71 ± 0.14	44.8 ± 1.7	129.2 ± 5.7	25.0
dAGTG**C**GATC								
rUGAG**A**GUAC	6.87 ± 0.44	72.1 ± 3.3	210.4 ± 10.0	38.4	6.91 ± 0.08	69.3 ± 4.5	201.1 ± 14.5	38.8
dACTC**C**CATG								
rUUGG**A**CACC	6.54 ± 0.88	67.7 ± 4.5	197.1 ± 13.5	37.2	6.64 ± 0.18	62.4 ± 3.1	179.8 ± 10.1	37.5
rA·dG mismatches								
rAAGC**A**GUAG	5.38 ± 0.18	66.1 ± 2.0	195.6 ± 6.0	31.9	5.38 ± 0.52	59.7 ± 2.2	175.1 ± 8.0	31.2
dTTCG**G**CATC								
rUCAC**A**CUAG	4.94 ± 0.06	51.2 ± 0.9	149.1 ± 2.8	27.8	4.85 ± 0.07	53.4 ± 2.1	156.6 ± 6.9	27.4
dAGTG**G**GATC								
rUGAG**A**GUAC	6.59 ± 0.89	83.8 ± 7.5	248.8 ± 22.6	37.4	6.91 ± 0.70	79.1 ± 7.0	232.8 ± 22.1	38.4
dACTC**G**CATG								
rUUGG**A**CACC	7.59 ± 0.30	54.8 ± 2.1	152.2 ± 6.0	43.2	7.59 ± 0.08	49.7 ± 2.5	135.7 ± 7.8	43.9
dAACC**G**GTGG								
rC·dA mismatches								
rAAGC**C**GUAG	5.08 ± 0.08	58.0 ± 1.2	170.6 ± 3.7	29.5	5.15 ± 0.13	56.7 ± 2.7	166.2 ± 9.0	29.6
dTTCG**A**CATC								
rUCAC**C**CUAG	ND[d]	ND	ND		ND	ND	ND	
dAGTG**A**GATC								
rUGAG**C**GUAC	5.84 ± 0.49	67.9 ± 3.5	200.2 ± 10.5	33.7	5.90 ± 0.09	66.1 ± 1.7	194.1 ± 5.4	34.1
dACTC**A**CATG								
rUUGG**C**CACC	ND	ND	ND		ND	ND	ND	
dAACC**A**GTGG								
rC·dT mismatches								
rAAGC**C**GUAG	5.27 ± 0.94	61.5 ± 5.0	181.2 ± 15.1	30.9	5.27 ± 0.15	61.1 ± 1.6	179.9 ± 1.6	30.9
dTTCG**T**CATC								
rUCAC**C**CUAG	ND	ND	ND		ND	ND	ND	
dAGTG**T**GATC								
rG·dA mismatches								
rAAGC**G**GUAG	5.35 ± 0.25	63.3 ± 2.4	186.7 ± 7.3	31.5	5.49 ± 0.15	58.4 ± 2.1	170.5 ± 6.9	31.7
dTTCG**A**CATC								
rUCAC**G**CUAG	4.30 ± 0.14	49.3 ± 1.5	145.1 ± 4.7	23.6	4.20 ± 0.17	51.1 ± 1.9	151.1 ± 6.5	23.7
dAGTG**A**GATC								
rUGAG**G**GUAC	6.95 ± 0.42	73.5 ± 3.3	214.6 ± 9.8	38.8	6.78 ± 0.46	76.7 ± 1.9	225.3 ± 6.3	38.2
dACTC**A**CATG								
rUUGG**G**CACC	6.80 ± 0.07	61.9 ± 1.0	177.6 ± 3.1	38.4	7.01 ± 0.15	56.2 ± 2.3	158.6 ± 7.4	39.7
dAACC**A**GTGG								
rG·dG mismatches								
rAAGC**G**GUAG	5.89 ± 0.54	73.6 ± 3.9	218.2 ± 11.7	34.5	5.81 ± 0.20	72.5 ± 2.5	214.9 ± 8.0	34.1
dTTCG**G**CATC								
rUCAC**G**CUAG	5.28 ± 0.17	64.2 ± 1.9	190.0 ± 6.0	31.0	5.20 ± 0.09	67.0 ± 2.7	199.2 ± 8.7	31.0
dAGTG**G**GATC								
rUGAG**G**GUAC	7.38 ± 0.68	85.1 ± 4.6	250.7 ± 14.0	40.0	7.40 ± 0.11	85.5 ± 4.5	252.0 ± 14.8	40.0
dACTC**G**CATG								
rUUGG**G**CACC	8.25 ± 0.40	61.9 ± 2.7	173.1 ± 7.8	45.7	8.26 ± 0.10	58.2 ± 3.6	161.1 ± 11.9	46.4
dAACC**G**GTGG								

Table 1 (Continued)

RNA/DNA duplex	T_m^{-1} vs log C_t parameters				curve fit parameters			
	$-\Delta G°_{37}$ (kcal/mol)	$-\Delta H°$ (kcal/mol)	$-\Delta S°$ (cal/mol·K)	T_m[b] (C)	$-\Delta G°_{37}$ (kcal/mol)	$-\Delta H°$ (kcal/mol)	$-\Delta S°$ (cal/mol·K)	T_m[b] (C)
rG·dT mismatches								
rAAGC**G**GUAG dTTCG**T**CATC	8.62 ± 0.17	73.8 ± 1.8	210.0 ± 5.2	46.3	8.51 ± 0.15	71.0 ± 1.8	201.4 ± 5.6	46.0
rUCAC**G**CUAG dAGT**T**GATC	6.83 ± 0.21	63.1 ± 1.9	181.4 ± 5.8	38.5	6.91 ± 0.35	66.3 ± 5.7	191.5 ± 18.4	38.8
rG·dT mismatches								
rUGAG**G**GUAC dACT**C**CATG	8.82 ± 0.10	75.6 ± 1.2	215.4 ± 3.8	44.6	8.90 ± 0.10	73.9 ± 3.5	209.5 ± 11.3	47.4
rUUG**G**CACC dAAC**T**GTGG	9.53 ± 0.65	61.8 ± 3.5	168.5 ± 9.7	52.9	9.53 ± 0.23	64.6 ± 4.4	177.6 ± 13.7	52.0
rUCUAC**G**CAG dAGAT**T**GTC	6.42 ± 0.82	67.0 ± 5.8	195.5 ± 17.3	36.2	6.51 ± 0.25	64.4 ± 5.6	186.6 ± 18.5	37.0
rUUA**G**ACUGGC dAAT**T**TGACCG	7.95 ± 0.86	66.3 ± 5.5	188.0 ± 15.9	44.0	7.96 ± 0.12	70.4 ± 5.5	201.2 ± 17.7	43.6
rUUAA**G**CUGGC dAATT**T**GACCG	8.93 ± 0.23	69.8 ± 2.0	196.2 ± 5.9	48.1	8.84 ± 0.13	66.0 ± 3.6	184.3 ± 11.2	48.2
rUUAAC**G**UGGC dAATTG**T**ACCG	8.51 ± 0.09	68.7 ± 11.2	194.1 ± 33.5	46.2	8.43 ± 0.09	63.5 ± 3.8	177.4 ± 11.9	46.8
rUUAACU**G**GGC dAATTGA**T**CCG	8.21 ± 0.77	75.3 ± 4.6	216.3 ± 13.4	44.1	8.17 ± 0.13	70.8 ± 2.9	201.8 ± 9.1	44.5
rU·dC mismatches								
rAAGC**U**GUAG dTTCG**C**CATC	5.33 ± 0.35	57.4 ± 2.8	167.8±8.3	30.8	5.60 ± 0.38	53.3 ± 4.3	153.8 ± 12.8	31.7
rUCAC**U**CUAG dAGTG**C**GATC	4.80 ± 0.48	40.1 ± 2.6	114.0 ± 7.5	23.8	4.95 ± 0.27	37.2 ± 2.7	104.1 ± 9.4	24.1
rUGAG**U**GUAC dACT**C**CATG	5.55 ± 0.06	67.7 ± 1.1	200.3 ± 3.6	32.7	5.49 ± 0.55	63.6 ± 8.1	187.4 ± 26.9	32.0
rUUG**U**CACC dAAC**C**GTGG	5.74 ± 0.20	61.9 ± 2.0	181.0 ± 6.1	33.2	5.89 ± 0.14	60.0 ± 2.6	174.5 ± 8.5	33.7
rU·dG mismatches								
rAAGC**U**GUAG dTTCG**G**CATC	6.39 ± 0.37	76.7 ± 3.6	226.8 ± 10.8	36.3	6.44 ± 0.27	69.6 ± 4.8	203.7 ± 16.2	36.5
rUCAC**U**CUAG dAGTG**G**GATC	5.59 ± 0.19	65.2 ± 2.0	192.1 ± 6.2	32.7	5.50 ± 0.04	68.1 ± 1.2	201.7 ± 3.8	32.6
rUGAG**U**GUAC dACTC**G**CATG	6.99 ± 0.53	72.1 ± 3.6	209.9 ± 10.7	39.0	7.01 ± 0.08	69.5 ± 2.8	201.4 ± 9.1	39.3
rUUG**U**CACC dAAC**G**GTGG	8.22 ± 0.40	65.9 ± 2.7	186.0 ± 7.8	45.1	8.19 ± 0.14	61.0 ± 2.3	170.2 ± 7.5	45.8
rUGUAG**U**GAC dACATC**G**CTG	7.16 ± 0.28	74.7 ± 2.5	217.6 ± 7.6	39.9	7.20 ± 0.07	80.0 ± 5.5	234.7 ± 17.7	39.7
rUUA**U**ACUGGC dAAT**G**TGACCG	7.42 ± 0.48	63.3 ± 3.4	180.1 ± 9.9	41.5	7.49 ± 0.08	61.6 ± 5.6	174.6 ± 18.2	41.7
rUUAA**U**CUGGC dAATT**G**GACCG	7.42 ± 0.23	87.2 ± 2.6	257.2 ± 8.0	40.2	7.49 ± 0.10	79.6 ± 4.3	232.5 ± 14.1	40.8
rUUAAC**U**UGGC dAATTG**G**ACCG	6.76 ± 0.48	76.3 ± 8.4	224.2 ± 31.3	38.0	6.81 ± 0.22	76.4 ± 8.0	224.4 ± 25.3	38.1
rUUAACU**U**GGC dAATTGA**G**CCG	6.63 ± 0.29	76.4 ± 2.8	225.0 ± 8.4	37.4	6.56 ± 0.09	77.3 ± 3.6	228.1 ± 11.8	37.1
rU·dT mismatches								
rAAGC**U**GUAG dTTCG**T**CATC	ND	ND	ND		ND	ND	ND	
rUCAC**U**CUAG dAGTG**T**GATC	4.06 ± 0.28	49.5 ± 2.1	146.5 ± 6.3	22.3	4.27 ± 0.22	47.0 ± 3.1	137.6 ± 10.7	23.1
rUGAG**U**GUAC dACT**C**TCATG	5.68 ± 0.40	82.6 ± 3.5	248.0 ± 10.8	33.9	5.78 ± 0.21	78.6 ± 7.1	234.7 ± 23.6	34.2
rUUG**U**CACC dAAC**T**GTGG	6.22 ± 0.11	56.6 ± 1.3	162.6 ± 3.8	35.0	6.06 ± 0.26	61.1 ± 3.3	177.4 ± 10.9	34.7

[a] All experiments were conducted in a buffer containing 1 M NaCl/10 mM Na_2HPO_4/1 mM Na_2EDTA, pH 7.0. [b] T_m calculated for 10^{-4} M total strand concentration. [c] Data from Sugimoto et al. (1995) *Biochemistry*, *34*, 11211−11215. [d] ND, not determined.

helical structure and thermodynamics of rG·dA or rA·dG mismatches in rAAGCNGUAG/dCTACN′GCTT, rUCACNCUAG/dCTAGN′GTGA, rUGAGNGUAC/dGTACN′CTCA, and rUUGGNCACC/dGGTGN′CCAA. Figure 1, panels A and B, show CD spectra of rUUGGACACC/dGGTGGCCAA and rUUGGGCACC/dGGTGACCAA measured at pH 5.0, 6.0, and 7.0. The spectrum of rUUGGACACC/dGGTGGCCAA was altered by pH, and the intensity of the maximum peak at ∼265 nm decreased and shifted from 265 nm (at pH 7.0) to 269 nm (at pH 5.0) with isodichroic points at 275 and 252 nm. In contrast, no pH effect was observed for rUUGGGCACC/dGGTGACCAA as well as a duplex without mismatch nucleotides of rUUGGACACC/dGGTGTCCAA (data not shown). The pH-dependent structural

Table 2: Thermodynamics of Duplex Formation of of RNA/DNA Hybrids Containing an Internal G·U or G·T Mismatch Base Pair[a]

	T_m^{-1} vs log C_t parameters				curve fit parameters			
RNA/DNA duplex	$-\Delta G°_{37}$ (kcal/mol)	$-\Delta H°$ (kcal/mol)	$-\Delta S°$ (cal/mol·K)	T_m[b] (°C)	$-\Delta G°_{37}$ (kcal/mol)	$-\Delta H°$ (kcal/mol)	$-\Delta S°$ (cal/mol·K)	T_m[b] (°C)
rAAGC**G**GUAG dTTCG**U**CATC	8.14 ± 0.35	71.3 ± 2.7	203.7 ± 8.0	44.1	8.17 ± 0.07	74.0 ± 3.0	212.1 ± 9.5	44.2
rUCAC**G**CUAG dAGTG**U**GATC	6.72 ± 0.34	70.4 ± 3.0	205.2 ± 9.0	38.0	6.79 ± 0.09	64.3 ± 1.4	185.3 ± 4.6	38.5
rUGAG**G**GUAC dACTC**U**CATG	8.64 ± 0.39	77.5 ± 3.0	221.9 ± 9.0	45.8	8.70 ± 0.12	78.9 ± 1.7	226.5 ± 5.5	45.6
rUUGG**G**CACC dAACC**U**GTGG	9.06 ± 0.30	69.7 ± 2.3	195.6 ± 6.8	48.6	8.94 ± 0.09	64.7 ± 1.7	179.7 ± 5.4	49.1
rAAGC**(dU)**GUAG dTTCG **G** CATC	5.85 ± 0.05	62.4 ± 0.9	182.3 ± 2.8	33.7	5.73 ± 0.10	65.9 ± 2.3	194.1 ± 7.6	33.1
rUCAC**(dU)**CUAG dAGTG **G** GATC	4.94 ± 0.20	57.4 ± 1.9	169.2 ± 5.9	28.5	4.89 ± 0.11	58.2 ± 2.1	172.0 ± 7.0	28.3
rUGAG**(dU)**GUAC dACTC **G** CATG	6.36 ± 0.22	63.6 ± 2.1	184.6 ± 6.2	36.1	6.44 ± 0.12	62.3 ± 6.2	179.8 ± 20.4	36.5
rUUGG**(dU)**CACC dAACC **G** GTGG	7.63 ± 0.26	57.4 ± 2.0	160.5 ± 5.7	43.0	7.65 ± 0.14	54.0 ± 4.3	149.4 ± 13.8	43.6
rAAGC**(dT)**GUAG dTTCG **G** CATC	6.22 ± 0.07	57.7 ± 1.0	166.0 ± 3.1	35.3	6.09 ± 0.48	53.9 ± 2.2	154.2 ± 7.9	34.4
rUCAC**(dT)**CUAG dAGTG **G** GATC	5.04 ± 0.22	60.5 ± 2.2	179.0 ± 6.6	29.3	5.20 ± 0.15	57.2 ± 2.2	167.8 ± 7.6	29.7
rUGAG**(dT)**GUAC dACTC **G** CATG	6.76 ± 0.28	76.4 ± 2.8	224.6 ± 8.4	37.9	6.79 ± 0.08	74.3 ± 0.4	217.8 ± 1.2	37.9
rUUGG**(dT)**CACC dAACC **G** GTGG	7.94 ± 0.11	63.3 ± 1.2	178.4 ± 3.6	44.2	7.95 ± 0.25	59.4 ± 3.5	165.8 ± 10.6	44.7

[a] All experiments were conducted in a buffer containing 1 M NaCl/10 mM Na_2HPO_4/1 mM Na_2EDTA, pH 7.0. [b] T_m calculated for 10^{-4} M total strand concentration.

changes were also observed for rAAGCAGUAG/dCTACGGCTT, rUCACACUAG/dCTAGGGTGA, and rUGAGAGUAC/dGTACGCTCA, in which a single rA·dG mismatch was present. However, all the duplexes containing an rG·dA mismatch examined showed no structural changes by pH (data not shown).

Figure 2 shows $\Delta G°_{37}$ values for G·A mismatches measured at several pH conditions. All rG·dA mismatches slightly (0.34 ∼ 0.04 kcal mol^{-1}) reduced the stability upon changing the pH from 7.0 to 5.0; however, all the duplexes containing rA·dG mismatches enhanced the stability by 0.13 ∼ 0.68 kcal mol^{-1}. The duplex without mismatch nucleotides of rUUGGACACC/dGGTGTCCAA reduced the stability by 0.39 kcal mol^{-1} at pH 5.0. Since UV melting curves for these duplexes proved to form stable duplexes under the CD measuring conditions, there are mechanisms for stabilizing only rA·dG mismatches with a slight alteration of the duplex structure.

Prediction Parameters of Trinucleotide in RNA/DNA Mismatches. Thermodynamic parameters to predict Watson−Crick base pairs in RNA (*1*, *11*, *17*), DNA (*2*, *13*, *15*), and RNA/DNA duplexes (*12*) have been reported based on the nearest-neighbor model (*49*). The model has also been applied to RNA and DNA duplexes containing single or tandem mismatches (*15*, *16*, *18*−*35*). Because it was not known whether the nearest-neighbor model could be applied for single mismatches in RNA/DNA duplexes, we examined trinucleotides containing the mismatch and adjacent base pairs that affected the mismatch stabilities as described above. Two duplexes of rUCACGCUAG/dCTAGTGTGA and rUCUACGCAG/dCTGTGTAGA which include a rG·dT mismatch between two adjacent rC/dG base pairs are composed of the same units of rUC/dGA, rCA/dTG, rAC/dGT, rCGC/dGTG, rCU/dAG, rUA/dTA, and rAG/dCT. Although the locations of the mismatch were different, UV melting experiments revealed similar thermodynamics for these duplexes such as −64.7 and −65.7 kcal mol^{-1} for $\Delta H°$, −186.5 and −191.1 cal mol^{-1} K^{-1} for $\Delta S°$, and −6.87 and −6.47 kcal mol^{-1} for $\Delta G°_{37}$, respectively. Another pair of rUGAGUGUAC/dGTACGCTCA and rUGUAGUGAC/dGTCGCTACA containing an rU·dG mismatch also showed similar thermodynamics (−70.8 and −77.4 kcal mol^{-1} for $\Delta H°$, −205.7 and −226.2 cal mol^{-1} K^{-1} for $\Delta S°$, and −7.00 and −7.18 kcal mol^{-1} for $\Delta G°_{37}$, respectively). These results suggest that the trinucleotide model is valid for comparing the stability of single mismatches in RNA/DNA duplexes.

Figure 3, panels A−C, summarize thermodynamics for all RNA/DNA trinucleotides examined in this study, although thermodynamics for rC·dA and rC·dT mismatches could not be determined due to their low stabilities. The most stable mismatch pair was rG·dT ($\Delta G°_{37} = -2.47 \sim -3.43$ kcal mol^{-1}) which could form stable wobble base pairs as reported for rG·rU and dG·dT mismatches (*36*, *37*). The least stable mismatches were rU·dC, rU·dT, and rA·dA ($\Delta G°_{37} = -0.6 \sim +1.1$ kcal mol^{-1}), likely the consequence of the unfavorable stacking interactions and backbone distortions at the mismatch sites. However, larger stability enhancements were observed for other purine−purine mismatches of rG·dA, rA·dG, and rG·dG, and these are the same mismatches that we found to form stable hydrogen bond structures in RNA and DNA duplexes (*32*, *35*, *38*−*41*, *50*). The overall trend averaged over all contexts at 37 °C was rG·dT ≫ rU·dG ≈ rG·dG > rA·dG ≈ rG·dA ≈ rA·dC > rA·dA ≈ rU·dT ≈ rU·dC > rC·dA ≈ rC·dT, although the order could be slightly altered by the identity of the adjacent base pairs. The order of adjacent base pairs was found to be rGNC/

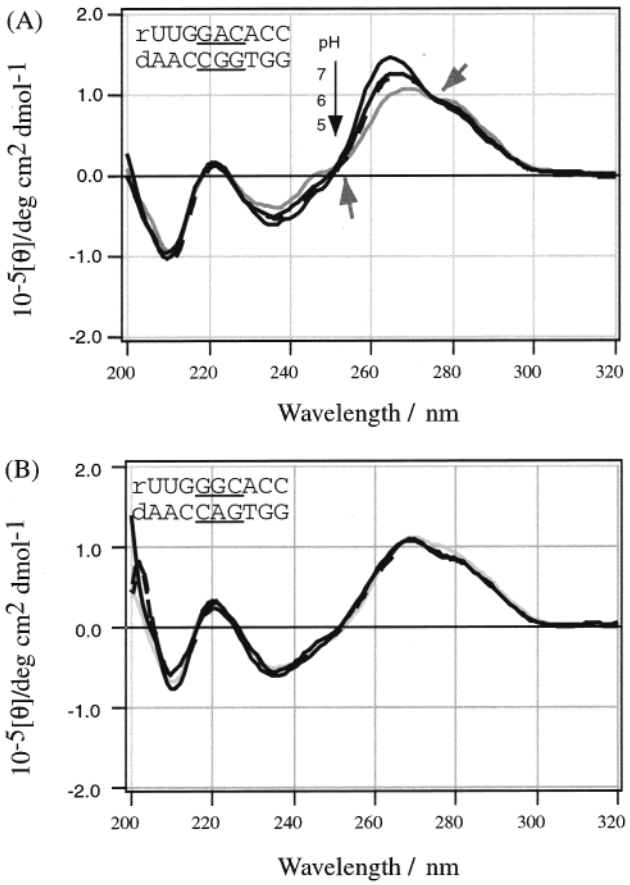

FIGURE 1: Effects of pH on CD spectra of (A) rA·dG and (B) rG·dA mismatches in RNA/DNA duplexes; (A) rUUGGACACC/dGGTGGCCAA and (B) rUUGGGCACC/dGGTGACCAA. Isodichoric points are pointed by gray arrows. Each oligomer concentration was 70 μM, and measurements were done in 1 M NaCl-phosphate buffer at pH 7.0 (black line), pH 6.0 (dotted line), and pH 5.0 (gray line) at 5 °C.

dGN′C > rGNG/dCN′C > rCNC/dGN′G > rCNG/dCN′G. These parameters are useful to predict RNA/DNA duplex stabilities containing single mismatch sites.

DISCUSSION

Stability−Structure Relationship for Single Mismatches in RNA/DNA Duplexes. In this study, general features of single mismatches have been investigated by comparing with the results of RNA and DNA duplexes previously reported. The order of the trinucleotide stability in RNA/DNA duplexes was approximately rG·dT ≫ rU·dG ≈ rG·dG > rA·dG ≈ rG·dA ≈ rA·dC > rA·dA ≈ rU·dT ≈ rU·dC > rC·dA ≈ rC·dT. Similar trends are reported for single mismatches in DNA (*35*) and RNA duplexes (*23*), suggesting that in general single G·T, G·U, G·G, and G·A mismatches are relatively stable and T·C, U·C, A·C, and C·C are less so. The nature of the adjacent base pairs considerably influenced the trinucleotide parameters except for rU·dC, rU·dT, and rA·dA mismatches as shown in Figure 3A. Since rU·dC, rU·dT, and rA·dA were found to be unstable mismatches, this suggests that they form mostly unstacked conformations, which would not have preference for the adjacent base pairs. This might be also true for rC·dT mismatches of which the thermodynamics could not be determined due to their instability. These observations are reasonable given the

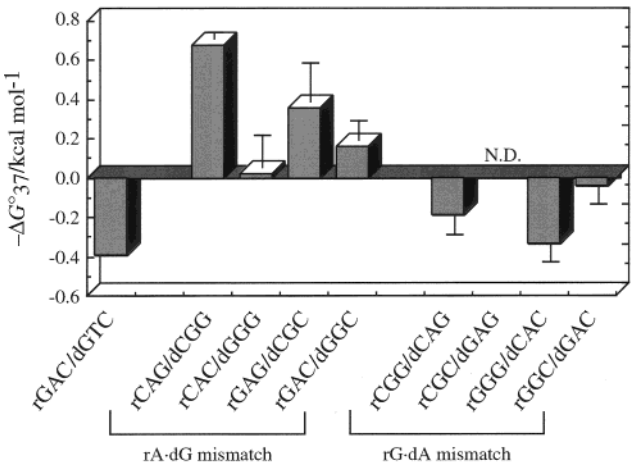

FIGURE 2: Increments of the free energy at 37 °C ($\Delta\Delta G°_{37}$) for rA·dG and rG·dA mismatches in RNA/DNA duplexes from pH 7.0 to pH 5.0. The sequences represented as a trinucleotide sequence are rAAGCNGUAG/dCTACN′GCTT, rUCACNCUAG/dCTAGN′GTGA, rUGAGNGUAC/dGTACN′CTCA, and rUUGGNCACC/dGGTGN′CCAA, where rN·dN′ is either rG·dA or rA·dG mismatch. Thermodynamics for rUCACGCUAG/dCTAGAGTGA could not be determined because of low stability (ND).

constraints of a canonical helical structure (C1′−C1′ distance of 10.4 ∼ 10.7 Å for Watson−Crick base pairs) to insert the mismatch nucleotides in the center of a helix.

In contrast to rA·dA mismatches, other purine−purine mismatches of rG·dA, rA·dG, and rG·dG appeared to have preferential adjacent base pairs, and all of these pairs are found to form hydrogen bonds in RNA and DNA duplexes (*32*, *35*, *38*−*41*, *50*). Four types of conformations are reported for A·G single mismatches (*32*, *38*−*41*); A(*anti*)·G(*anti*) which utilizes the imino proton of guanine for a hydrogen bond (C1′−C1′ distance is 12.8 ∼ 13.0 Å), A(*anti*)·G(*anti*) which makes hydrogen bonding between the N7 nitrogen atom and an exocyclic amine to give a sheared form (C1′−C1′ distance of 9.1 Å), A(*syn*)·G(*anti*) (C1′−C1′ distance of ∼10.7 Å), and A^+(*anti*)·G(*syn*) at low pH (∼10.7 Å). The C1′−C1′ distance for imino and sheared A·G pairs would not be accommodated to a constricted single mismatch environment, although these are often found for tandem G·A mismatches in RNA duplexes (*39*, *40*) that have wider helical grooves to accommodate the *anti*−*anti* mismatch conformations. It is speculated that single purine−purine mismatches in DNA duplexes are favored to form anti−syn conformations to reduce the distortion at the backbone (*38*, *51*, *52*). In fact, A(*syn*)·G(*anti*) and A^+(*anti*)·G(*syn*) which can be accommodated in a B-form structure are found for single dG·dA mismatches in DNA duplexes (*53*, *54*). Figures 1 and 2 show the pH-dependent structural and thermodynamic changes for G·A mismatches in RNA/DNA duplexes. With these results, we considered the geometry of G·A pairs in RNA/DNA duplexes despite the fact that it was difficult to estimate the structure only with the CD spectra. Because all rA·dG mismatches showed a higher thermostability as well as CD spectra changes at low pH, A^+(*anti*)·G(*syn*) form might be dominant at low pH. Since anticonformations are favorable in guanine for a stronger stacking interaction with adjacent base pairs, guanine in an RNA strand might prefer to form an anticonformation. Thus, it is likely that rG·dA mismatches preferentially formed an A(*syn*)·G(*anti*) conformation such that pH affected less on both stability and

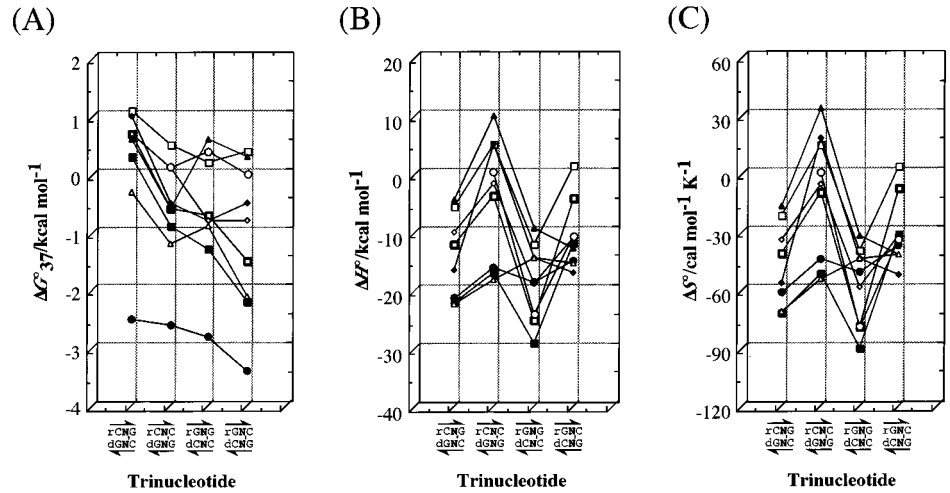

FIGURE 3: Comparison of thermodynamic parameters of (A) $\Delta G°_{37}$, (B) $\Delta H°$, and (C) $\Delta S°$ for the trinucleotide formations containing rA·dA (□), rA·dC (◆), rA·dG (□), rG·dA (◇), rG·dG (■), rG·dT (●), rU·dC (▲), rU·dG (△), or rU·dT (○), respectively. Estimated errors in $\Delta G°_{37}$, $\Delta H°$, and $\Delta S°$ are ±0.22 kcal mol^{-1}, ±3 kcal mol^{-1}, and ±8 cal mol^{-1} K^{-1}, respectively.

structure as observed for a duplex of rUUGGACACC/dGGTGTCCAA that does not contain mismatches.

The rG·dG mismatches in RNA/DNA duplexes showed relatively higher stability than rG·rG mismatches in DNA and RNA duplexes (*23*, *35*). The G(*syn*)·G(*anti*) pairs with a rapid conformational exchange are reported for single dG·dG mismatches that can fit to B-form DNA duplexes (*35*, *50*). Thus, rG·dG mismatches would be stable due to the ability to form G(*syn*)·G(*anti*) pairs that do not affect the backbone structure. Purine−pyrimidine mismatches can be stacked in a helix without disrupting adjacent base pairs as seen for G·U and G·T wobble base pairs that have a C1′−C1′ distance of 10.8 Å of the C1′−C1′ distance, agreeing with those of Watson−Crick base pairs. The dA·dC mismatches are reported to form two hydrogen bonds at low pH (*34*, *55*−*57*), but the stability enhancements of rC·dA mismatches appeared low, perhaps due to the dominant unprotonated form of adenine at pH 7.0 examined here. Nevertheless, some rA·dC mismatches showed slight stability enhancements at pH 7.0, likely due to favorable stacking interactions for the mismatch pair or the perturbation of pK_a of adenine which would be affected by the environment (*58*).

The ranges of $\Delta H°$ and $\Delta S°$ for trinucleotides were from +9.9 to −29.0 kcal mol^{-1} and from +33.8 to −89.7 cal mol^{-1} K^{-1}, respectively. Since $\Delta H°$ and $T\Delta S°$ for Watson−Crick base pairs highly compensated each other ($r^2 \sim 0.99$) (*59*), the ratio of $T\Delta S°/\Delta H°$ would reflect the $\Delta H°$ and $\Delta S°$ contributions on the helical stability. The $T\Delta S°/\Delta H°$ values ranged from 0.76 to 0.86 for rA·dT, rU·dA, rG·dC, and rC·dG Watson−Crick base pairs at the rN·dN′ positions of duplexes, and these values were significantly smaller than all mismatches examined here (on the average 0.94) except for rG·dT mismatches (0.77 ∼ 0.88). This observation suggests that rG·dT mismatches can form stable hydrogen bonding sufficient to compensate for the entropic loss in a base pair formation as Watson−Crick base pairs do.

In Figure 3B, rCNG/dCN′G and rGNG/dCN′C showed larger negative enthalpy changes than rCNC/dGN′G and rGNC/dGN′C trinucleotides. This is not the same trend as found for $\Delta G°_{37}$ but rather is consistent with $\Delta H°$ values of nearest-neighbor interactions in the adjacent base pairs: −16.3, −12.8, −9.3, and −8.0 kcal mol^{-1} for rCG/dCG, rGG/dCC, rCC/dGG, and rGC/dGC, respectively. This observation was also found for $T\Delta S°$ in Figure 3C. Therefore, $\Delta H°$ and $\Delta S°$ of mismatches appeared to be proportional to those of Watson−Crick base pairs. Two explanations are possible for the observation. Perhaps the mismatches are flipped out, and the adjacent base pairs can interact with each

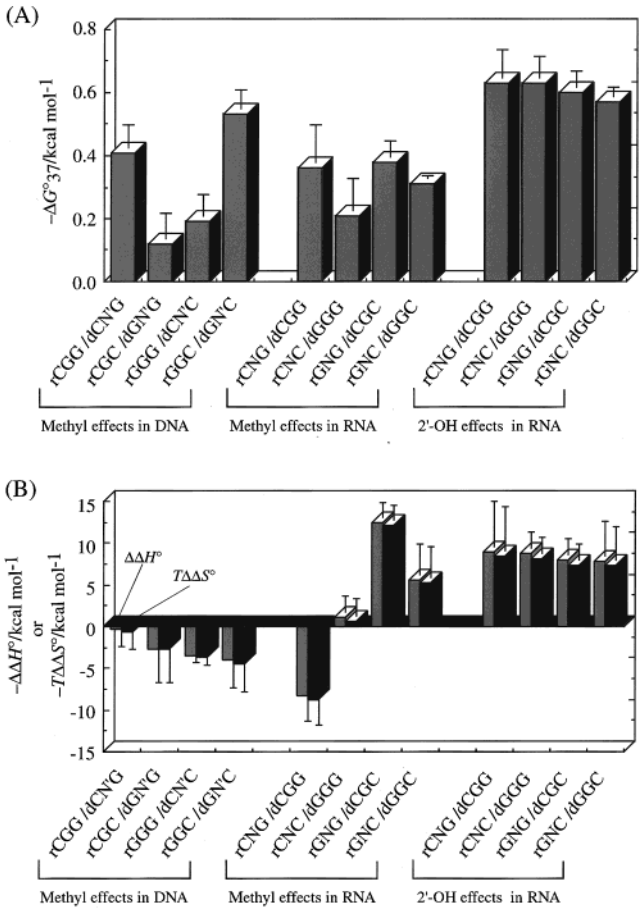

FIGURE 4: Increments of the stability by the replacement of uracil by thymine in G·U mismatches that adds the methyl group to C5 of uracil. The methyl group is added to either an RNA or a DNA strand (rN or dN′). The energies of the 2′-hydroxyl group in ribouridine (rN) are also compared. Thermodynamic parameters used here are (A) $\Delta\Delta G°_{37}$ and (B) $\Delta\Delta H°$ and $T\Delta\Delta S°$ at 37 °C.

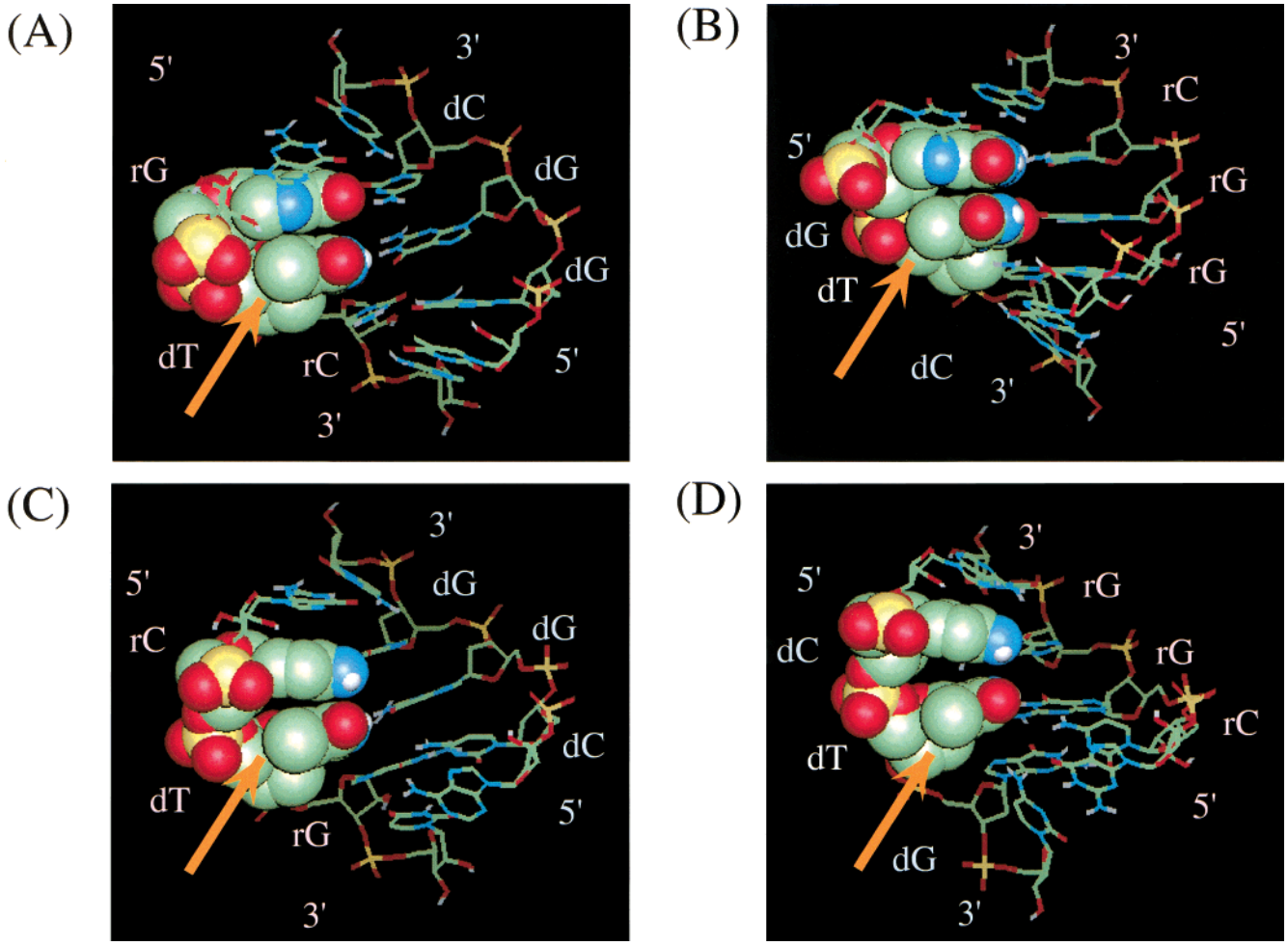

FIGURE 5: Molecular modeling for (A) rG(dT)C/dGGC, (B) rGGC/dCTG, (C) rC(dT)G/dCGG, and (D) rCGG/dGTC calculated by QUANTA 97.1/CHARMm version 23.2. Arrows indicate the C5-methyl group in G·T mismatches. The methyl group in the dT·dG mismatch overlaps to the 5′-guanine on the same strand.

other. However, since an RNA/DNA duplex containing an abasic site (F) of rAAGCUGUAG/dCTACFGCTT was too unstable to measure the thermodynamics (data not shown), stable interactions between the adjacent base pairs appear unlikely. Another explanation is that the strength of the interaction in the trinucleotides correlated to the stability of the closing base pairs. This possibility is discussed later.

Energy Contributions from the Methyl Group in Thymine and the 2′-Hydroxyl Group to the Wobble Base Pair Stability. To characterize the difference of the stability for rG·dU and rT·dG mismatches in RNA/DNA duplexes, we substituted the bases in the Wobble base pairs. Replacements of rG·dT by rG·dU and dT·dG by dU·dG remove the methyl group from C5 of the thymine and the replacement of rU·dG by dU·dG removes the 2′-hydroxyl group from the uridine. The removal of the 2′-hydroxyl group from a ribonucleotide introduced a deoxyribose into an RNA strand to form an RNA−DNA chimeric strand. However, since we have shown that $\Delta G°_{37}$ for duplexes having RNA−DNA chimeric junctions can be predicted based on the nearest-neighbor model (*60*), the 2′-hydroxyl group would influence only the nearest-neighbor interaction.

Stability enhancements by the methyl group and the 2′-hydroxyl group additions in the mismatches are compared in Figure 4 A. The methyl group stabilized duplexes by 0.12 ∼ 0.53 kcal mol^{-1} depending on the flanking base pair as discussed later. The energy increments due to the methyl group of thymine are similar to values reported previously for Watson−Crick base pairs (0.18 and 0.28 kcal mol^{-1}) (*61*). Methyl groups are supposed to stabilize duplexes by enhancing stacking and hydrophobic interactions (*62*, *63*). However, the origin of the stabilization was different depending on the strand in which the methyl group was introduced. Addition of the methyl group to rGUG/dCGC and rGUC/dGGC stabilized the duplex by the $\Delta H°$ contributions, where the methyl group is supposed to enhance the stacking interaction as well as the hydrophobic interaction. In contrast, other cases stabilized the duplex by the $T\Delta S°$ contributions, which implies the methyl group predominantly enhances the hydrophobic interaction (Figure 4B). Molecular modeling in Figure 5 suggested the $\Delta H°$ contributions for the methyl group incorporation to uracil next to 5′-guanine in an RNA strand.

Because thermodynamics ($\Delta G°_{37}$, $\Delta H°$, and $\Delta S°$) obtained by the 2′-hydroxyl group were unaffected by the identity of the flanking base pair, the 2′-hydroxyl group in ribouridine was unlikely to interact directly with adjacent base pairs. The 2′-hydroxyl group enhanced the stability by 0.57 ∼ 0.63 kcal mol^{-1}, and the stabilization originated mainly from the enthalpy contributions. The favorable enthalpy change for the 2′-hydroxyl groups may be the interaction with O_4' in the same strand (*44*) or a conformational change driven by

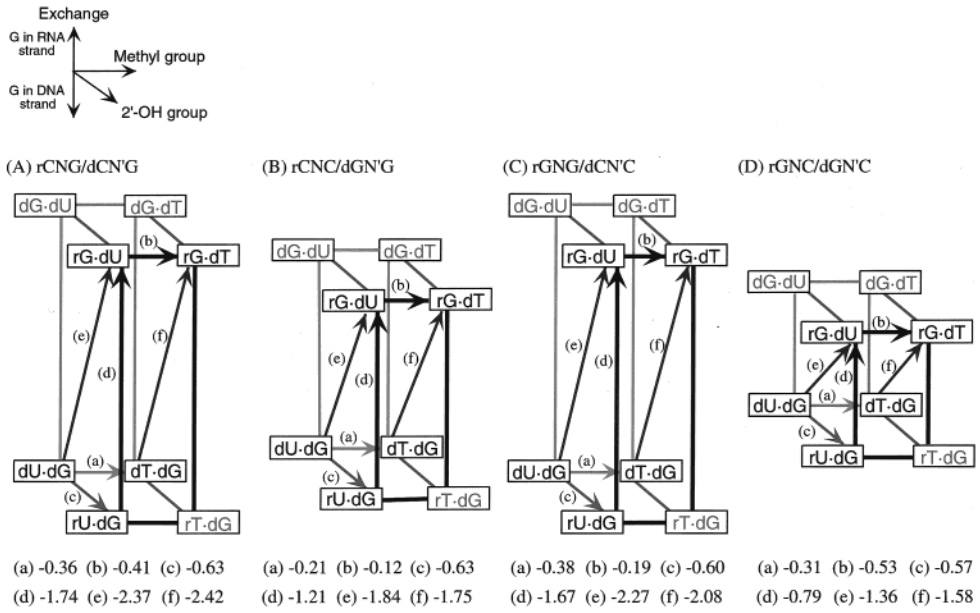

FIGURE 6: Increments of the free energy of trinucleotides by the replacements of (a) dU·dG replacements by dT·dG (methyl group addition in an RNA strand), (b) rG·dU replacements by rG·dT (methyl group addition in a DNA strand), (c) dU·dG replacements by rU·dG (2′-hydroxyl group addition to deoxyuridine), (d) rU·dG replacements by rG·dU (nucleotide exchange), (e) dU·dG replacements by rG·dU (base exchange and 2′-hydroxyl group addition), and (f) dT·dG replacements by rG·dT (base exchange and 2′-hydroxyl group addition). The $\Delta G°_{37}$ values are determined independently. Estimation errors are ±0.22 kcal mol^{-1}. The rT·dG, dG·dU, and dG·dT mismatches not measured in this study are included to identify the replacements of five mismatches examined here.

the 2′-hydroxyl group to alter the sugar puckers from C2′-endo to C3′-endo (*46*).

The energy cost required for the removal of the methyl group from thymine and the 2′-hydroxyl group from ribouridine can be roughly estimated by the comparison of the reported nearest-neighbor parameters containing rU/dA and dT/dA base pairs. The differences of the nearest-neighbor stabilities between RNA/DNA duplexes (rUA/dTA, rUC/dGA, and rUG/dCA) and DNA duplexes (dTA/dTA, dTC/dGA, and dTG/dCA) are 0.0 ∼ 0.3 kcal mol^{-1} (rUU/dAA is omitted because of an unusual stability) (*12*, *13*). These differences are similar to those of the stability between rU·dG and dT·dG mismatches (0.22 ∼ 0.43 kcal mol^{-1}).

Substitutions at the G·T mismatch examined here were (a) dU·dG replacements by dT·dG (methyl group addition in an RNA strand), (b) rG·dU replacements by rG·dT (methyl group addition in a DNA strand), (c) dU·dG replacements by rU·dG (2′-hydroxyl group addition to deoxyuridine in an RNA strand), (d) rU·dG replacements by rG·dU (nucleobase exchange), (e) dU·dG replacements by rG·dU (nucleobase exchange and the 2′-hydroxyl group addition), and (f) dT·dG replacements by rG·dT (base exchange and 2′-hydroxyl group addition in an RNA strand). Figure 6 summarizes the trinucleotide stability enhancements of the (a)−(f) replacements measured independently. Imaginary mismatches of rT·dG, dG·dU, and dG·dT were also included that are not measured in this study. Increased energy by the methyl group addition to r<u>CNG</u>/d<u>CN′G</u> and r<u>CNC</u>/d<u>GN′G</u> trinucleotides were not very different regardless of which strand the methyl group was incorporated (−0.36 and −0.41 kcal mol^{-1} for r<u>CNG</u>/d<u>CN′G</u>, and −0.21 and −0.12 kcal mol^{-1} for r<u>CNC</u>/d<u>GN′G</u>). However, the effects of the methyl group on r<u>GNG</u>/d<u>CN′C</u> and r<u>GNC</u>/d<u>GN′C</u> differed depending on which strand the methyl group was incorporated; the incorporation of a methyl group to the RNA strand enhanced the stability by 0.19 and 0.38 kcal mol^{-1} more than the case when it is added to the DNA strand. These results are consistent with the molecular models shown in Figure 5. Since G·T wobble bases are projected toward a minor and a major groove, respectively, the methyl group at C5 of thymine considerably overlaps with 5′-guanine that could gain the stacking interactions. Moreover, an RNA strand in RNA/DNA duplexes preferentially forms an A-form structure that has shorter intrahelical distances than a DNA strand that has longer intrahelical distances due to an interconversion between C2′-*endo* and C3′-*endo* sugar puckers (*46*); thus the stacking interaction by the methyl group might be stronger when it is introduced into an RNA strand. These favorable stacking interactions would be the parts of the origin of the $\Delta H°$ contribution for r<u>GUG</u>/d<u>CGC</u> and r<u>GUC</u>/d<u>GGC</u> stabilities.

It is interesting that the energies for the pathways (e) and (f) in Figure 6 were the same within an experimental error. This observation implies that increased stabilities by the methyl group addition were unaffected by the nucleotide exchanges. Thermodynamics from the 2′-hydroxyl group in the Wobble base pairs were also unaffected by the identity of adjacent base pairs. Moreover, the enhancement energies through the pathway (e) were the same as the total energy of the 2′-hydroxyl group addition (c) and the nucleotide exchanges (d). It was reported that the substitutions of the methyl group at C5 in thymine and 2′-hydroxyl groups are energetically independent of Watson−Crick base pairs (*61*). With these results, it is concluded that the energy enhancements by the methyl group of the thymine, the 2′-hydroxyl group of the ribouridine, and nucleotide exchanges in the wobble base pairs were independent. Because these energies could be treated additively, stabilities of the imaginary rT·dG, dG·dU, and dG·dT mismatches would be estimated from the diagram in Figure 6. The most dominant replacements on the stability were the nucleotide exchanges in the mismatches, which would predominantly alter the stacking

interaction. The difference between rU·dG and rG·dT was relatively larger (−1.74 and −1.67 kcal mol^{-1}) for unstable trinucleotides of rCNG/dCN′G and rGNG/dCN′C (−0.32 and −0.90 kcal mol^{-1} for a trinucleotide stability), while relatively smaller influences by the nucleotide exchange were observed (−1.21 and −0.79 kcal mol^{-1}) for stable rCNC/dCN′G and rGNC/dGN′C trinucleotides (−1.25 and −2.11 kcal mol^{-1}). These results suggest that guanine to interacts with adjacent base pairs stronger than thymine and uracil due to the larger aromatic system and polalizability. Since the interhelical distances of an RNA strand in RNA/DNA duplexes are supposed to be shorter than that of a DNA strand, a mismatched nucleotide inserted in an RNA strand may interact more strongly than a nucleotide in a DNA strand. Thus, the favorable stacking interactions for guanine in an RNA strand might be the origin of higher stabilities for rG·dT than rU·dG mismatches.

Comparison of Trinucleotide Parameters for RNA/DNA Duplexes with Those of RNA and DNA Duplexes. Although considerable amounts of thermodynamic data for single mismatches in RNA and DNA duplexes have been reported, the data are not complete for single mismatches to estimate all trinucleotide combinations except for rG·rU mismatches in RNA duplexes (*23*) and dG·dT mismatches in DNA duplexes (*15*). To investigate the relationship among the mismatch stabilities in RNA, DNA, and RNA/DNA duplexes, the stability of rG·rU and dG·dT mismatches were compared to those of Watson−Crick base pairs. There are 16 possible trinucleotides for rG·rU and dG·dT mismatches that can be calculated by reported nearest-neighbor parameters. A linear free energy relationship (LFER) was found for seven trinucleotides that include a dG·dT mismatch with dG·dC base pairs (*15*). We expanded the LFER to all possible mismatches in RNA, DNA, and RNA/DNA duplexes. Figure 7A shows linear correlations among the stabilities of all possible 16 kinds of rG·rU or dG·dT mismatches and corresponding rG·rC or dG·dC base pairs. Thus, the stability enhancements for dG·dT and rG·rU mismatches were proportional to the corresponding rG·rC and dG·dC Watson−Crick base pairs, and the mismatch stabilities for RNA duplexes were invariably more stable than those for DNA duplexes when the same trinucleotides were compared. In contrast to RNA and DNA duplexes, a nonlinear correlation was observed for RNA/DNA mismatches, although these stabilities were intermediate of these of RNA and DNA duplexes. There appeared to be a threshold for the RNA/DNA plots that classified the stability into those near RNA duplex stability (mostly for rG·dT mismatches) and those near DNA duplex stability (mostly for rU·dG mismatches) as shown in Figure 7A. This observation indicates that mismatched stability of rG·dT and rU·dG are proportional to those for the corresponding G·C Watson−Crick base pairs, implying the stacking interaction of guanine to be the main determining factor for the trinucleotide stability as well as for the Watson−Crick base pairs.

To elucidate the relationship among mismatch stabilities in RNA, DNA, and RNA/DNA duplexes, we calculated the relative stabilities of RNA/DNA mismatches to the stabilities of RNA and DNA duplexes that had the same trinucleotides. Figure 7B shows a correlation between mismatch stability in RNA/DNA duplexes and a fractional stability of RNA/DNA mismatches as compared to RNA and DNA mismatches. A good linear correlation in Figure 7B suggests that stable RNA/DNA mismatches (rG·dT mismatches) exhibit similar stabilities to those of RNA mismatches whereas unstable RNA/DNA mismatches (rU·dG mismatches) have analogous stabilities to those of DNA mismatches regardless of rG·dT and rU·dG mismatches. Since RNA and DNA duplexes generally form A-form and B-form structures that have mean interhelical distances of 2.56 and 3.38 Å, respectively (*44*), RNA/DNA duplexes may change the duplex structure depending on the duplex stability. This is reasonable if the equilibrium of the sugar puckers in a DNA strand between C2′-*endo* and C3′-*endo* affects the duplex stability. Shorter mean distance between nearest-neighbor bases can enhance the duplex stability, because it makes stronger stacking interactions from London dispersion contributions. Although the short distance of the nearest-neighbor bases would increase the electrostatic repulsion between phosphate groups, the stacking interaction might be overcome if more cations can shield the electrostatic repulsion of phosphates to form more stable duplexes (*64*, *65*).

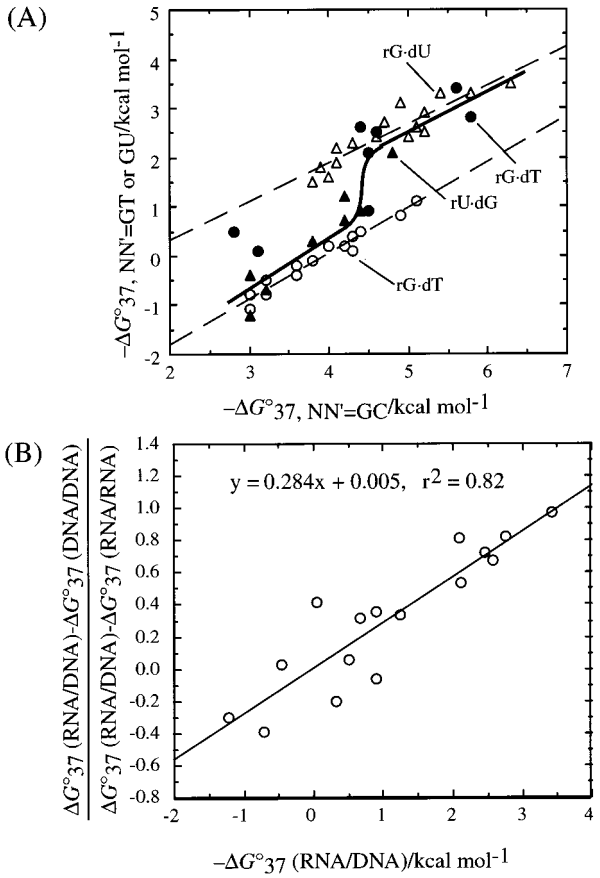

FIGURE 7: Relationship of the mismatch stabilities in RNA, DNA, and RNA/DNA duplexes. (A) Correlation of $\Delta G°_{37}$ values among dG·dT, dG·dU, rG·rU, and dG·dT mismatches and corresponding G·C Watson−Crick base pairs. (B) Correlation between mismatch stability in RNA/DNA duplexes and a fractional stability of mismatches of RNA/DNA as compared with mismatch stabilities in RNA and DNA duplexes.

ACKNOWLEDGMENT

We thank Professor Fu-Ming Chen, Tennessee State University, for a critical reading of the manuscript and helpful comments.

REFERENCES

1. Mathews, D. H., Sabina, J., Zuker, M., and Turner, D. H. (1999) *J. Mol. Biol. 288*, 911−940.
2. SantaLucia, J., Jr. (1998) *Proc. Natl. Acad. Sci. U.S.A. 95*, 1460−1465.
3. Goodman, M. F., Creighton, S., Bloom, L. B., and Petruska, J. (1993) *Crit. Rev. Biochem. Mol. Biol. 28*, 83−126.
4. Saiki, R. K., Gelfand, D. H., Stoffel, S., Scharf, S., Higuchi, R. H., Horn, G. T., Mullis, K. B., and Erlich, H. A. (1988) *Science 239*, 487−494.
5. Mirzabekov, A. D. (1994) *Trends Biotechnol. 12*, 27−32.
6. Strobel, S. A., Ortoleva-Donnelly, L., Ryder, S. P., Cate, J. H., and Moncoeur, E. (1998) *Nat. Struct. Biol. 5*, 60−66.
7. Ohmichi, T., and Sugimoto, N. (1997) *Biochemistry 36*, 3514−3521.
8. Pley, H, W., Flaherty, K. M., and Mckay, D. B. (1994) *Nature 372*, 68−74.
9. Battiste, J. L., Mao, H., Rao, N. S., Tan, R., Muhandiram, D. R., Kay, L. E., Frankel, A. D., and Williamson, J. R. (1996) *Science 273*, 1547−1551.
10. Su, L., Radek, J. T., Hallenga, K., Hermanto, P., Chan, G., Labetos, L. A., and Weiss, M. A. (1997) *Biochemistry 36*, 12722−12732.
11. Turner, D. H., Sugimoto, N., and Freier, S. M. (1988) *Annu. Rev. Biophys. Biophys. Chem. 17*, 167−192.
12. Sugimoto, N., Nakano, S., Katoh, S., Matsumura, A., Nakamuta, H., Ohmichi, T., Yoneyama, M., and Sasaki, M. (1995) *Biochemisty 34*, 11211−11216.
13. Sugimoto, N., Nakano, S., Yoneyama, M., and Honda, K. (1996) *Nucleic Acids Res. 24*, 4501−4505.
14. Owczarzy, R., Vallone, P. M., Gallo, F. J., Paner, T. M., Lane, M. J., and Benight, A. S. (1997) *Biopolymers 44*, 217−239.
15. Allawi, H. T., and SantaLucia, J., Jr. (1997) *Biochemistry 36*, 10581−10594.
16. Johnson, T., Zhu, J., and Wartell, R. M. (1998) *Biochemistry 37*, 12343−12350.
17. Xia, T., SantaLucia, J., Jr., Burkard, M. E., Kierzek, R., Schroeder, S, J., Jiao, X., Cox, C., and Turner, D. H. (1998) *Biochemistry 37*, 14719−14735.
18. Sugimoto, N., Kierzek, R., Freier, S. M., and Turner, D. H. (1986) *Biochemistry 25*, 5755−5759.
19. Morse, S. E., and Draper, D. E. (1995) *Nucleic Acids Res. 23*, 302−306.
20. Zhu, J., and Wartell, R. M. (1997) *Biochemistry 36*, 15326−15335.
21. Bevilacqua, J. M., and Bevilacqua, P. C. (1998) *Biochemistry 37*, 15877−15884.
22. Meroueh, M., and Chow, C. S. (1999) *Nucleic Acids Res. 27*, 1118−1125.
23. Kierzek, R., Burkard, M. E., and Turner, D. H. (1999) *Biochemistry 38*, 14214−14223.
24. SantaLucia, J., Jr., Kierzek, R., and Turner D. H. (1991) *J. Am. Chem. Soc. 113*, 4313−4322.
25. SantaLucia, J., Jr., Kierzek, R., and Turner D. H. (1991) *Biochemistry 30*, 8242−8251.
26. He, L., Kierzek, R., SantaLucia, J., Jr., Walter, A. E., and Turner, D. H. (1991) *Biochemistry 30*, 11124−11132.
27. Walter, A. E., Wu, M., and Turner, D. H. (1994) *Biochemistry 33*, 11349−11354.
28. Wu, M., McDowell, J., and Turner, D. H. (1995) *Biochemistry 34*, 3204−3211.
29. McDowell, J. A., and Turner, D. H. (1996) *Biochemistry 35*, 14077−14089.
30. Xia, T., McDowell, J., and Turner D. H. (1997) *Biochemistry 36*, 12486−12497.
31. Ke, S. H., and Wartell, R. M. *Biochemistry* (1995) *34*, 4593−4600.
32. Allawi, H. T., and SantaLucia, J., Jr. (1998) *Biochemistry 37*, 2170−2179.
33. Allawi, H. T., and SantaLucia, J., Jr. (1998) *Nucleic Acids Res. 26*, 2694−2701.
34. Allawi, H. T., and SantaLucia, J., Jr. (1998) *Biochemistry 36*, 9435−9444.
35. Peyret, N., Seneviratne, P. A., Allawi, H. T., and SantaLucia, J., Jr. (1999) *Biochemistry 38*, 3468−3477.
36. Sussman, J. L., Holbrook, S. R., Warrant, R. W., Church, G. M., and Kim, S. H. (1978) *J. Mol. Biol. 123*, 607−630.
37. Brown, T., Leonard, G. A., Booth, E. D., and Chambers, J. (1989) *J. Mol. Biol. 207*, 455−457.
38. Brown, T., Hunter, W. N., Kneale, G., and Kennard, O. (1986) *Proc. Natl. Acad. Sci. U.S.A. 83*, 2402−2406.
39. Wu, M., and Turner, D. H. (1996) *Biochemistry 35*, 9677−9689.
40. Wu, M., SantaLucia, J., Jr., and Turner, D. H. (1997) *Biochemistry 36*, 4449−4460.
41. Pan, B., Mitra, S. N., and Sandaralingam, M. (1999) *Biochemistry 38*, 2826−2831.
42. Gao, X., and Patel. D. J. (1987) *J. Biol. Chem. 262*, 16973−16984.
43. Brown, T., Leonard, G. A., and Booth, E. D. (1990) *J. Mol. Biol. 212*, 437−440.
44. Saenger, W. (1984) *Principles of Nucleic Acid Structure*, p 123, Springer-Verlag, New York.
45. Gyi, J. I., Conn, G. L., Lane, A. N., and Brown, T. (1996) *Biochemistry 35*, 12538−12548.
46. Gyi, J. I., Lane, A. N., Conn, G. L., and Brown, T. (1998) *Biochemistry 37*, 73−80.
47. Richards, E. G. (1975) *Handbook of Biochemistry and Molecular Biology*: *Nucleic Acids*, 3rd ed., *1*, p 597, CRC Press, Cleveland, UK.
48. Petersheim, M., and Turner, D. H. (1983) *Biochemistry 22*, 256−263.
49. Tinoco, I., Jr., Uhlenbeck, O. C., and Levine, M. D. (1971) *Nature 230*, 362−367.
50. Lane, A. N., and Peck, B. (1995) *Eur. J. Biochem. 230*, 1073−1087.
51. Webster, G. D., Sanderson, M. R., Skelly, J. V., Swann, P. F., Li, B. F., and Tickel, I. J. (1990) *Proc. Natl. Acad. Sci. U.S.A. 87*, 6693−6697.
52. Hunter, W. N., Brown, T., and Kennard, O. (1986) *J. Biomol. Struct. Dyn. 4*, 173−191.
53. Brown, T., Leonard, G. A., Booth, E. D., and Chambers, J. (1989) *J. Mol. Biol. 207*, 455−457.
54. Lane, A. N., Jenkins, T. C., Brown, D. J. S., and Brown, T. (1991) *Biochem. J. 279*, 269−281.
55. Boulard, Y., Cognet, J. A., Gabarro-Arpa, J., Le Bret, M., Carbonnaux, C. and Fazakerley, G. V. (1995) *J. Mol. Biol. 246*, 194−208.
56. Bhaumik, S. R., Chary, K. V., Govil, G., Liu, K., and Miles, H. T. (1997) *Biopolymers 41*, 773−784.
57. Jang, S. B., Hung, L. W., Chi, Y. I., Holbrook, E. L., Carter, R. J., and Holbrook, S. R. (1998) *Biochemistry 37*, 11726−11731.
58. Legault, P., and Pardi, A. (1997) *J. Am. Chem. Soc. 119*, 6621−6628.
59. Nakano, S., Fujimoto, M., Hara, H., and Sugimoto, N. (1999) *Nucleic Acids Res. 27*, 2957−2965.
60. Sugimoto, N., and Nakano, S., manuscript in preparation.
61. Wang, S., and Kool, E. T. (1995) *Biochemistry 34*, 4125−4132.
62. Shcweitzer, B. A., and Kool, E. T. (1995) *J. Am. Chem. Soc. 117*, 1863−1872.
63. Lesnik, E. A., and Freier, S. M. (1998) *Biochemistry 37*, 6991−6997.
64. Sugimoto, N., Nakano, S., and Fujimoto, M. (1997) *Nucleic Acids Symp. Ser. 34*, 61−62.
65. Nakano, S., and Sugimoto, N., unpublished data.

BI000819P